THE INTERNATIONAL JOURNAL OF
DEVELOPMENTAL
BIOLOGY

# Calnexin is required for zebrafish posterior lateral line development

I-CHEN HUNG[1], BOR-WEI CHERNG[1], WEN-MING HSU[5,6,*] and SHYH-JYE LEE[1,2,3,4,5,*]

[1]Institute of Zoology, [2]Department of Life Science, [3]Center for Biotechnology, [4]Center for Systems Biology, [5]Research Center for Developmental Biology and Regenerative Medicine, National Taiwan University, Taipei and [6]Department of Surgery, National Taiwan University Hospital and National Taiwan University College of Medicine, Taipei, Taiwan, R.O.C.

**ABSTRACT** **The lateral line is a mechanosensory system in fish and amphibians to detect local water flow and pressure. Development of the posterior lateral line (PLL) originates from the migrating PLL primordium (PLLP). The PLLP deposits neuromasts on the trunk during migration to the tail. Molecular dissection revealed that PLL development is associated with genes mediating cell adhesion, morphogenesis, neurogenesis and development, but the regulatory signaling network is far from completion. To further investigate candidate regulatory genes for lateral line development, we found using whole-mount *in situ* hybridization that *calnexin*, an endoplasmic reticular (ER) calcium-binding protein gene, is expressed in PLL neuromasts. Knockdown of calnexin using antisense morpholino oligonucleotides resulted in a dose-dependent reduction in neuromasts and hair cells of the PLL. Using a transgenic *claudin b:gfp* line, we observed a notably reduced PLLP size, but no significant migration defect in *calnexin* morphants. Finally, we discovered that the reduced PLLP is associated with a reduction in cell proliferation and an increase in ER stress-dependent apoptosis. These results suggest that calnexin is essential for neuromast formation during lateral line development in the zebrafish.**

KEY WORDS: *zebrafish, calnexin, lateral line, neuromast, ER stress*

## Introduction

The lateral line is a mechanosensory system in fish and amphibians which detects local water flow and pressure (Montgomery *et al.*, 2000). A series of neuromasts form the lateral line. A neuromast is composed of mechanosensory hair cells and peripheral cells. These neuromasts form anterior and posterior branches which respectively extend to the head or migrate through the trunk (Metcalfe *et al.*, 1985). The posterior lateral line (PLL) system originates from a placode just posterior to the otic vesicle (Baker and Bronner-Fraser, 2001). The PLL placode appears at 18~20 h post-fertilization (hpf) and divides into two cell populations. One population differentiates into sensory neurons as PLL ganglia, and the other one generates a migrating primordium which deposits neuromasts periodically along its way to the tail (Gilmour *et al.*, 2004). Each neuromast is innervated by afferent and efferent neurons to deliver nerve impulses (Metcalfe *et al.*, 1985, Raible and Kruse, 2000). In the meantime, glial cells migrate along the axons to form myelinated PLL nerves (Brosamle and Halpern, 2002).

Development of the PLL involves cell migration, proliferation,

ning to be unraveled, it is still far from completion.

To further investigate candidate genes which may be involved in lateral line development, we screened gene expression patterns in the Zebrafish Information Network (http://zfin.org) and found *calreticulin*, a calcium binding protein gene, is expressed in the lateral line. We confirmed its expression in lateral line using whole-mount in situ hybridization (WISH). In addition, we also found one of its related genes, *calnexin* is expressed at the lateral line system. Calreticulin and calnexin have high functional and structural similarity. The amino sequence of zebrafish calnexin and calreticulin show 41% identity and 53% similarity. Both of them have been implicated in diverse functions in ER. They play important roles in glycoprotein protein folding as a lectin-like chaperon (Danilczyk *et al.*, 2000, Ou *et al.*, 1993). These proteins are also involved in regulation of intracellular $Ca^{2+}$ homoeostasis and ER $Ca^{2+}$ capacity (Bedard *et al.*, 2005). Calreticulin contains acidic and proline rich arm domain which is critical in calcium storage of ER (Nakamura *et al.*, 2001). Calnexin regulates intracellular $Ca^{2+}$

homeostasis by modulating functions of the sarco-endoplasmic reticulum calcium ATPase (SERCA) 2b via phosphorylation (Roderick *et al.*, 2000). Previous studies have shown that both calreticulin and calnexin are involved in other cellular processes, including immunity, cell adhesion, and development (Gold *et al.*, 2010, Michalak *et al.*, 2009). We observed that both *calreticulin* and *calnexin* are specifically expressed in the PLL primordium (PLLP) and neuromasts in zebrafish larvae. Knockdown of both genes by antisense morpholino oligonucleotides (MOs) inhibited PLL development. The loss of calnexin had a more-profound effect on lateral line development compared to that of *calreticulin* MOs. In addition, the loss of calnexin has also been shown to impair the nerve development and rhodopsin maturation in mice and fruit flies, respectively (Denzel *et al.*, 2002, Rosenbaum *et al.*, 2006). These findings imply a role of calnexin in neuronal related organ development. So here we focus on calnexin and further demonstrated that the effects of the *calnexin* MO on lateral line development is associated with its inhibition on cell proliferation
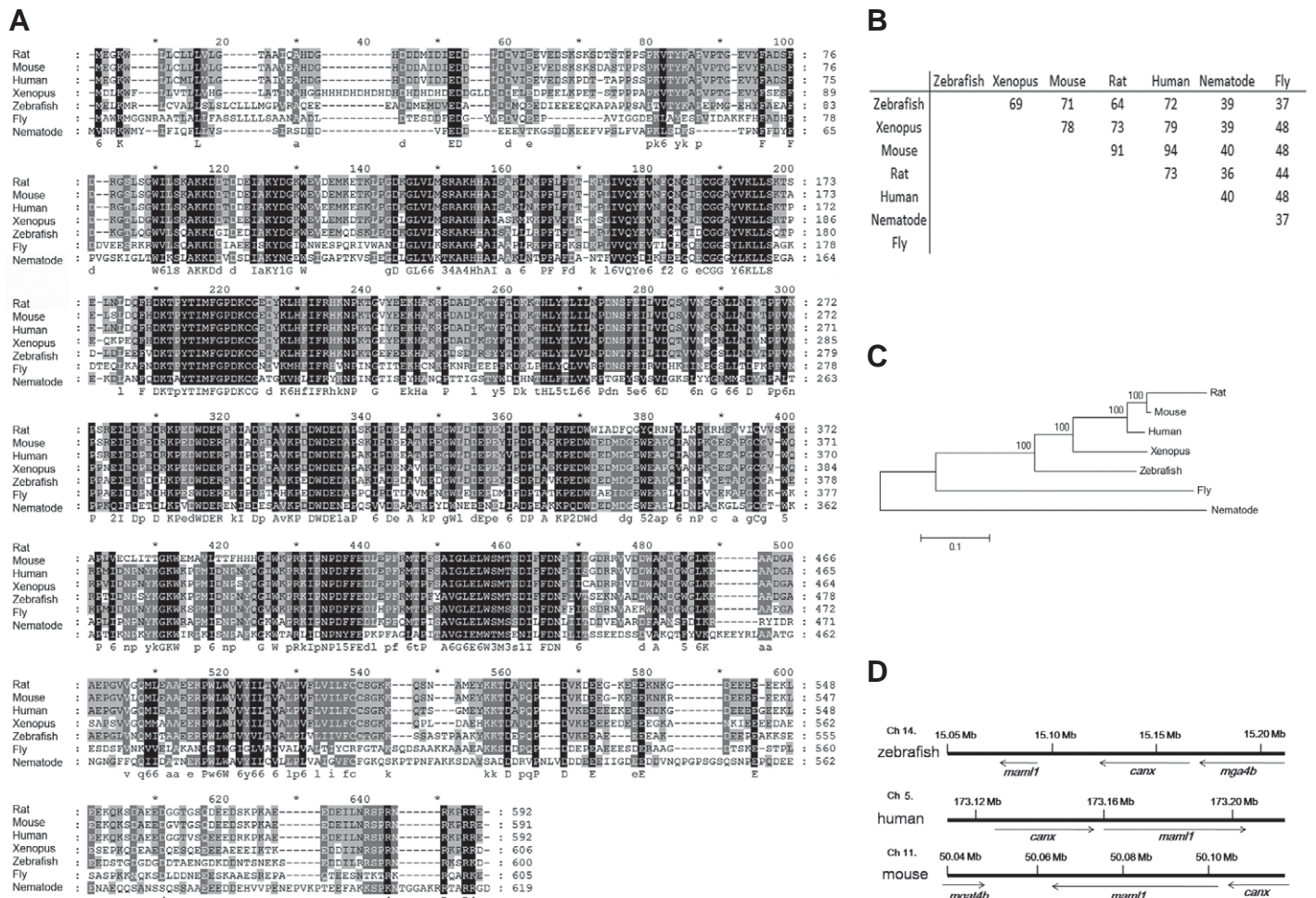
**B**

| | Zebrafish | Xenopus | Mouse | Rat | Human | Nematode | Fly |
|---|---|---|---|---|---|---|---|
| Zebrafish | | 69 | 71 | 64 | 72 | 39 | 37 |
| Xenopus | | | 78 | 73 | 79 | 39 | 48 |
| Mouse | | | | 91 | 94 | 40 | 48 |
| Rat | | | | | 73 | 36 | 44 |
| Human | | | | | | 40 | 48 |
| Nematode | | | | | | | 37 |
| Fly | | | | | | | |

**Fig. 1. Sequence analysis of zebrafish calnexin. (A)** *Multiple alignments of calnexin amino acid sequences of the rat (NM_172008.2), mouse (NM_007597.3), human (NM_001746.3), Xenopus laevis (NM_001085946.1), zebrafish (NM_213448.1), fruit fly (NM_170407.2), and nematode (NM_066775.3) by ClustalX. Identical amino acids across all and some species are respectively shaded in black and gray.* **(B)** *Identity table of calnexin amino acid sequences. Values represent percentages of identity between two species.* **(C)** *Phylogenic tree analysis of calnexins. The horizontal length indicates the estimated time that the sequence diverged from related family members. Multiple sequences were examined with ClustalX, using bootstrapping (500 reiterations), and the output tree was plotted by the Neighbor-joining method. The scale bar indicates the distance in units of fractions of amino acids differing between two sequences.* **(D)** *Synthetic analysis of calnexins. The resident chromosome for each calnexin is indicated. The orientation and comparable length of each gene are shown by arrows. Genes neighboring* calnexin *are also shown. Ch, chromosome; Mb, megabase.*

and an increase in ER stress-dependent apoptosis in PLLP.

## Results

### *Cloning and gene analysis*

To explore the role of calnexin in zebrafish development, we cloned a zebrafish calnexin gene by *in silico* cloning according to a NCBI reference sequence (NM_213448.1), which is the only zebrafish calnexin gene identified. The obtained zebrafish calnexin cDNA had 4220 base pairs (bp) with a coding region of 1803 bp, a 33-bp 5' untranslated region (UTR), and a 2384-bp 3' UTR. To compare the protein sequence homology of calnexin across species, the translated zebrafish calnexin amino acid sequence was aligned with its homologues in the human (*Homo sapiens*), rat (*Rattus norvegicus*), mouse (*Mus musculus*), African clawed toad (*Xenopus laevis*), fly (*Drosophila melanogaster*), and nematode (*Caenorhabditis elegans*) as shown in Fig. 1A. The amino acid sequence of zebrafish calnexin was highly conserved compared to its vertebrate homologues (human, mouse, rat, and African clawed toad) but not compared to those of invertebrate homologues (nematode and fly). Zebrafish calnexin had 72% identical and 85%

similar amino acids compared to its human homolog (see other comparisons in Fig. 1B). The evolutional distances of zebrafish calnexin to other calnexins are clearly shown in the phylogenetic trees (Fig. 1C). Zebrafish calnexin was placed in between, but was closer to vertebrate than to invertebrate homologues.

To further study gene conservation in vertebrate calnexins (zebrafish, human, and mouse), we obtained and compared their chromosome location maps from the Ensemble database (http://www.ensembl.org/index.html). All calnexin genes are located near *mgata4b* (*alpha-1, 3-mannosyl-glycoprotein 4-beta-N-acetylglucosaminyltransferase B*) and *maml1* (*mastermind-like 1*). The gene orientation of zebrafish *calnexin* is the same as that of mouse *calnexin* but is reverse to that of human *calnexin* (Fig. 1D).

### *Expression of calnexin in the zebrafish lateral line system*

To detect temporal and spatial expressions of *calnexin* in developing zebrafish, we used reverse-transcription polymerase chain reaction (RT-PCR) and WISH to analyze its expression patterns of early embryos, larvae, and different adult tissues. The RT-PCR analysis showed that *calnexin* transcripts appeared in 1-cell-stage embryos to 3 days post-fertilization (dpf) larvae, but was notably
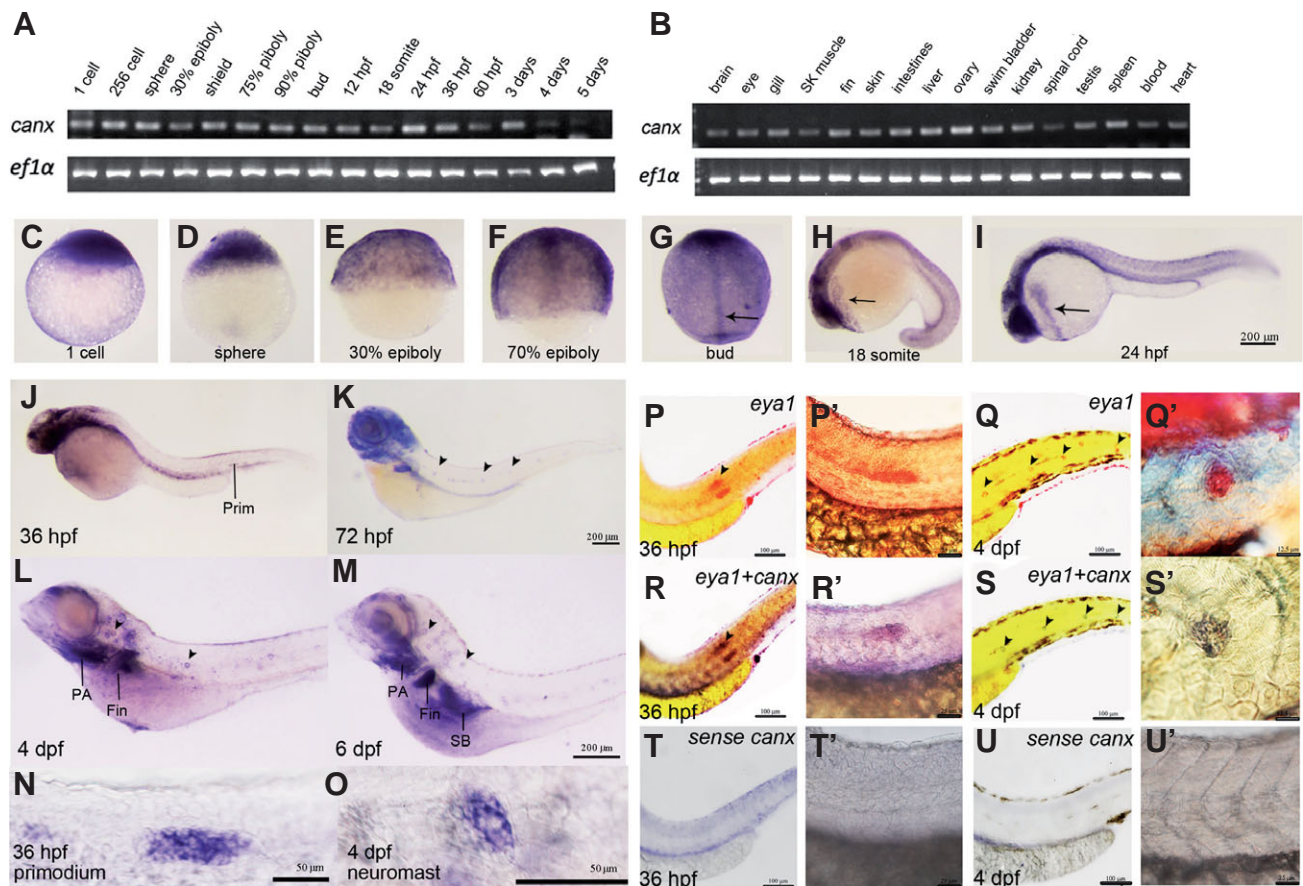


**Fig. 2. Spatial and temporal expression patterns of *calnexin* in developing zebrafish embryos.** *RT-PCR analyses of* calnexin *were performed using cDNAs from embryos at designated stages* **(A)** *and in different adult tissues* **(B)**. *A 107-bp* calnexin *fragment was amplified, and a 524-bp* ef1α *fragment was also amplified as an internal control.* **(C-U')** *Whole-mount in situ hybridization by a* calnexin *antisense riboprobe was performed in embryos at designated stages. All photographs shown are in lateral view except for F and G which are in dorsal view;* **(H-U')** *anterior to the left, dorsal to the top. Arrows indicate the notochord* **(G)** *and hatching gland* **(H, I)**. *Arrowheads point to selected neuromasts* **(K-M)**; *Large scale view of primordium* **(N)** *and neuromast* **(O)**. **(P-S)** *Co-expression assay* eya1 *and* canx. *Embryos were fixed at designated times and subjected to WISH against indicated genes. Arrows point to primordia in panels P and R and neuromasts in panels Q and S, respectively. Enlarged images are shown in panels P'-S'. hpf, hours post-fertilization; dpf, days post-fertilization; Prim, primordium; PA, pharyngeal arch; SB, swim bladder.*

reduced in 4~5-dpf larva (Fig. 2A). In addition, *calnexin* was expressed in all adult tissues examined (Fig. 2B).

To further investigate the spatial expression profile of *calnexin*, we performed WISH analyses and found that *calnexin* was ubiquitously expressed in embryos from the 1-cell stage to 30% epiboly stage (Fig. 2 C-E). Its expression domains were restricted to the head, hatching gland, and notochord from the 70% epiboly stage to 24 h post-fertilization (hpf) (Fig. 2 F-I). From 36 hpf to 6 dpf, *calnexin* expression domains were found at the pharyngeal arches (Fig. 2 K-M), fins (Fig. 2 K-M), and swim bladder (Fig. 2M) and showed up in a spot-like pattern at the lateral line primordium and neuromasts along the head to the truck axis (Fig. 2 J-O). To confirm the expres-
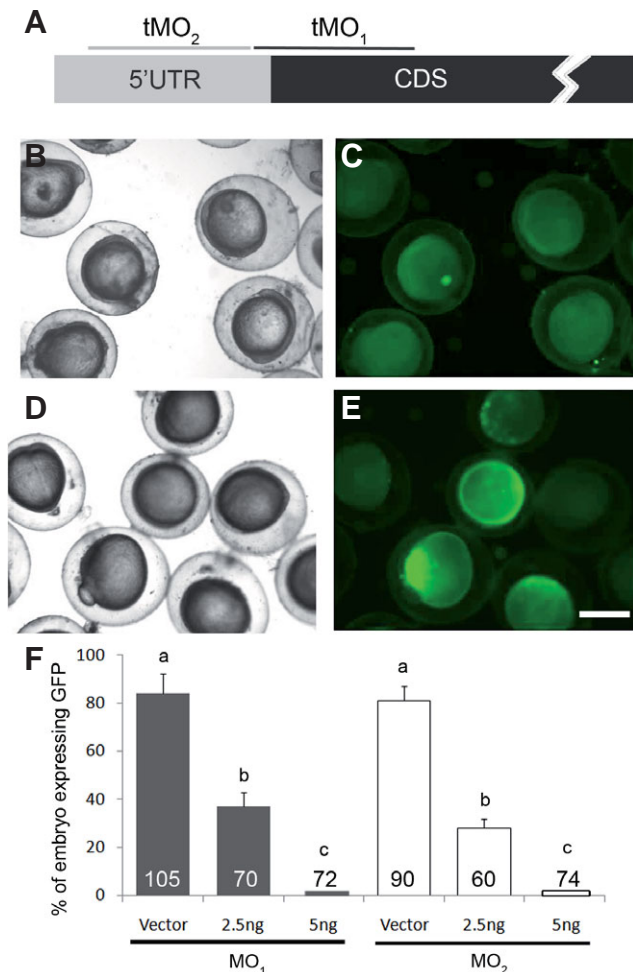
sion of *calnexin* in lateral line, we performed double WISH of *eya1*, a marker gene of neuromast, with *calnexin*. Results showed that *eya1* and *calnexin* co-expressed in neuromasts and PLLP (Fig. 2 P-S'). To ensure the specificity, we used a *calnexin* sense probe as a negative control and observed no staining in neuromasts (Fig. 2 T-U'). Collectively, these data demonstrate the presence of *calnexin* transcripts in the lateral line system.

The expression of *calnexin* in the lateral system suggests its potential role in regulating lateral line development and/or functions. We thus generated two translational blocking MOs (designated $MO_1$ and $MO_2$) against *calnexin*, which respectively targeted the start codon and the 5'UTR, as shown in Fig. 3A. To examine whether *calnexin* expression could be inhibited by the MOs, we inserted a stretch of *calnexin* nucleotides of ~200 bp, which contained the $MO_1$ target site, into a pCS2+ XLT vector with a green fluorescent protein (GFP) gene and co-injected 150 pg of this construct with 2.5 or 5 ng of $MO_1$. We observed and calculated percentages of embryos expressing GFP. Embryos injected without $MO_1$ showed a mosaic expression of GFP fluorescence ($84\% \pm 8\%$, $n = 105$) at 10 hpf (Fig. 3D,E), but the percent of GFP-expressing embryos was notably reduced in embryos co-injected with 2.5 ($37\% \pm 6\%$, $n = 70$) and 5 ng ($0\% \pm 0\%$, $n = 72$) $MO_1$ (Fig. 3 B,C). $MO_2$ was also examined as described and showed similar MO efficacy (Fig. 3F).

### Knockdown of calnexin causes a reduction in posterior lateral line neuromasts

The zebrafish lateral line system is composed of a series of neuromasts. Each neuromast consists of a cluster of pear-like hair cells surrounded by long, slender supporting cells. A sensing hair (kinocilium) is on top of the hair cell and projects into a jellylike cupula as shown in a schematic drawing (Fig. 4A). To reveal neuromasts, we used wheat germ agglutinin conjugated with Alexa Fluor 488 (WGA488) and (2-(4-(dimethylamino)styryl)-N-ethylpyridinium iodide) (DASPEI) to respectively stain the cupula and hair cells (Fig. 4B). In control embryos exposed to WGA488 only, distinct clusters of neuromasts derived from the anterior and posterior lateral lines were observed in the lateral line system along the trunk and head region (Fig. 4C). Similar pattern was observed in embryos injected with a standard control MO (Fig. 4D). *calnexin* MOs dose-dependently inhibited the formation of neuromasts as evidenced by the disappearance of WGA488-labeled cupula (Fig. 4 E-H). The dose-dependent inhibition of neuromast formation by *calnexin* MOs was best shown by counting the numbers of neuromasts that appeared on one side of the trunk region of 72-hpf embryos (Fig. 4I). To examine the specificity of the *calnexin* MO, embryos were co-injected with 5 ng $MO_1$ and 25 pg *calnexin* mRNAs. The neuromast numbers were significantly restored in *calnexin* morphants co-injected with *calnexin* mRNAs (Fig. 4I). Similar inhibition on neuromast formation was observed in embryos treated with two translational-blocking MOs against *calreticulin* (Fig. 5). However, the inhibition of *calreticulin* MOs was less effective even at a higher dosage (10 ng) used, so we decided to focus on calnexin hereafter.

To further investigate the effects of the *calnexin* MOs on neuromast formation, we examined the integrity of hair cells by DASPEI staining. Because there is no definite number of hair cells in each neuromast, we counted the total number of hair cells in the L1 to L3 neuromasts on the left side of the trunk (Harris *et al.*, 2003). *calnexin* MOs dose-dependently reduced the numbers of hair cells of L1-3 neuromasts, and the reduction was rescued by co-injecting

**Fig. 3. *Calnexin* morpholino oligonucleotide (MO) target sites and potency examination. (A)** *A partial mRNA map of* calnexin *is presented. Black and gray boxes represent part of the coding sequence (CDS) with an ATG translation initiation site and untranslated region (UTR), respectively. The* calnexin $MO_1$- *and* $MO_2$-*binding sites are indicated as shown. The potency of MO1 to reduce calnexin expression was shown by coinjecting 150 pg of the pCS2+-CANX-GFP-XLT plasmid with **(B,C)** or without **(D, E)** calnexin $MO_1$; then it was cultured, observed under a bright **(B,D)** or dark field through an FITC filter **(C,E)**, and photographed at 10 h post-fertilization (hpf). The percentage (%) of green fluorescent protein (GFP)-expressing embryos for each treatment is shown as the mean ± standard error in **(F)**. Different letters at the top of each column indicate a significant difference between groups at p < 0.05. Scale bar: 200 μm. The number within each column is the sample size.*

*calnexin* mRNAs (see representative photographs in Fig. 6A and quantitative analyses in Fig. 6B).

The *calnexin* MO at a higher dose (5 ng) caused a higher incidence of mortality in 3-dpf embryos. To rule out a possible off-target effect of MO-induced p53-depdendent apoptosis (Robu *et al.*, 2007), we co-injected the *calnexin* $MO_1$ with the *p53* MO. *calnexin* $MO_1$ caused a significant reduction in the survival rate compared to that of untreated embryos, and it could be partially rescued by the co-injection of 2.5 and 5 ng of the *p53* MO (Fig. 7C). In contrast, numbers of neither neuromasts nor hair cells were restored (Fig. 7 A,B). To monitor cell apoptosis, we used a vital dye, acridine orange, and observed that the apoptosis cell numbers dramatically increased in *calnexin* morphants with or without the *p53* MO (Fig. 7 D-F). These data suggest that the lateral line defects induced by *calnexin* MO were not p53-dependent.

### Knockdown of calnexin does not affect migration but reduces cell number of the PLLP

The reduction of primordium deposition might have been due to interference with PLLP migration. The PLLP is determined at 18~20 hpf and begins to migrate from the head region toward the tail at 40 hpf (Dambly-Chaudiere *et al.*, 2003). To monitor PLLP migration, we used a transgenic *claudin b:gfp* line (Haas and Gilmour, 2006), which expresses EGFP at the lateral line primordium and peripheral cells, to examine whether primordial migration was affected by the loss of calnexin. Embryos were injected with the StdMO or $MO_1$, incubated, and photographed at 30 and 36 hpf under epifluorescence microscopy (Fig. 8 A-D). We measured the migration path of the PLLP from the head to the tip of the primordium, and the body length. The PLLP migration distance-to-body length ratio did not significantly differ between StdMO- and *calnexin* MO-injected embryos (Fig. 8E). Furthermore, we noticed that the primordium size of *calnexin* morphants appeared to be smaller than that of control embryos. Thus, we classified *calnexin* morphants into three groups with normal, medium and severe-affected PLLP under confocal microscopy (Fig. 8 F-H). We found more than 70% of PLLP in *calnexin* morphants was smaller in size compared to less than 15% observed in that of control embryos (Fig. 8I). To examine whether the PLLP size reduction was due to the decrease in cell number, we used 4',6-diamidino-2-phenylindole (DAPI) to stain nuclei and quantified PLLP cell number in both control embryos and *calnexin* morphants under confocal microscopy (Fig. 8 J,K) . We observed
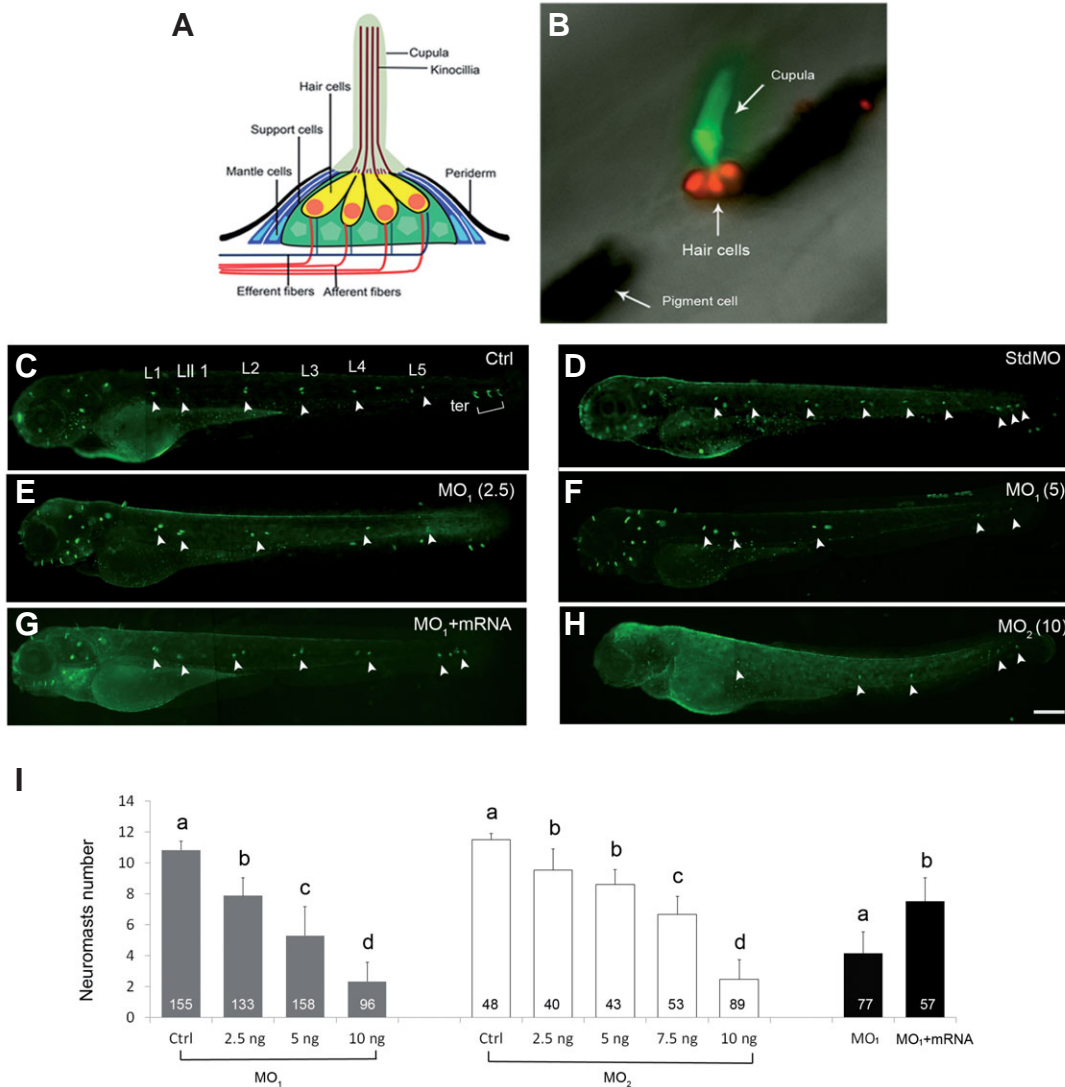


Fig. 4. Knockdown of calnexin dose-dependently inhibited the formation of neuromasts. (A) *Diagram of a fish neuromast (modified from (Ma and Raible, 2009).* (B) *A zebrafish neuromast was labeled by WGA 488 (green) and DASPEI (red) to respectively reveal its cupula and hair cells. Two large black patches are pigments.* (C-I) *Embryos were treated without or with indicated morpholino oligonucleotide (MO; ng/embryo) of a standard control MO (stdMO, 5 ng), calnexin $MO_1$ or calnexin $MO_2$, incubated until 3 days post-fertilization, stained with WGA 488, and observed and photographed under epifluorescence microscopy. calnexin mRNAs (25 pg) was added for MO rescue* (G). *Photographs are shown in lateral view with the anterior toward the left and posterior to the right. Only left side trunk neuromasts are indicated by white arrowheads. Trunk neuromasts are designated L1~ L5, LII1, and ter as shown in untreated larvae (C, Ctrl). The vague green fluorescent spots are out-of-focus neuromasts on the opposite side of the trunk. Numbers of left side neuromasts were counted* (I). *Different letters at the top of each column indicate a significant difference between groups at p < 0.05. Scale bar: 200 am. The number within each column is the sample size.*
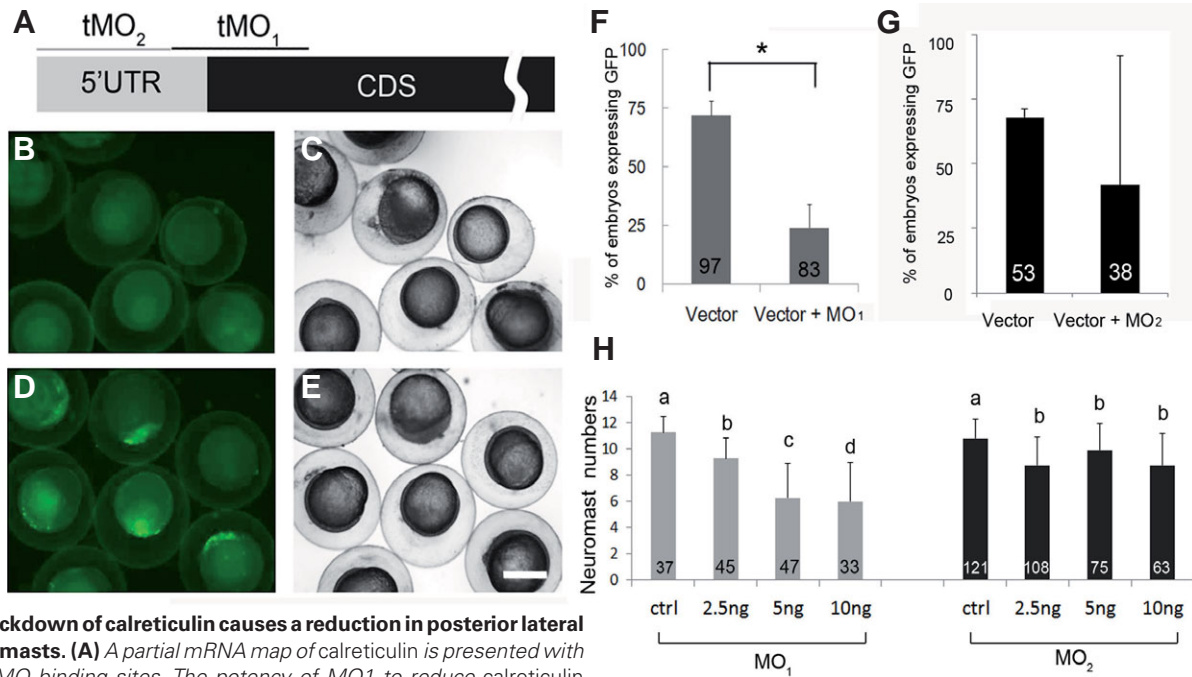
**Fig. 5. Knockdown of calreticulin causes a reduction in posterior lateral line neuromasts. (A)** *A partial mRNA map of* calreticulin *is presented with indicated MO binding sites. The potency of MO1 to reduce* calreticulin *expression was shown by co-injecting 150 pg of the pCS2+-CRT-GFP-XLT plasmid with* **(B,C)** *or without* **(D,E)** calreticulin *MO1; then it was cultured, observed under a bright* **(C,E)** *or dark field* **(B,D)**, *and photographed at 10 hpf. The percentage (%) of green fluorescent protein (GFP)-expressing embryos for 5ng calreticulin MO₁ or calreticulin MO₂ for each treatment is shown as the mean ± standard error in* **(F,G)**, *respectively. Embryos were treated, observed and shown as described previously. Numbers of neuromasts on the left side of the trunk in all treatments were counted and are shown in* **(H)**. *Different letters at the top of each column indicate a significant difference between groups at p < 0.05. Scale bar: 200 μm. The number within each column is the sample size.*

a significant reduction in PLLP cell number in *calnexin* morphants compared to that of control embryos (Fig. 8I).

### Loss of calnexin reduces cell proliferation and increases apoptosis in the PLLP

To study the reduction of primordium size in *calnexin* morphants, we examined whether their cell proliferation were affected. We performed BrdU and GFP immunohistochemistry in transgenic *claudin b:gfp* embryos to label proliferative cells and the PLLP, respectively. The number of BrdU-labeled cells in the PLLP was measured and calculated by the ImageJ software. PLLP proliferative cells in *calnexin* morphants were found to be significantly decreased compared to that of controlled embryos (Fig. 9 A,B). On the other hand, we stained cell nuclei with DAPI and examined apoptotic cells by a TUNEL
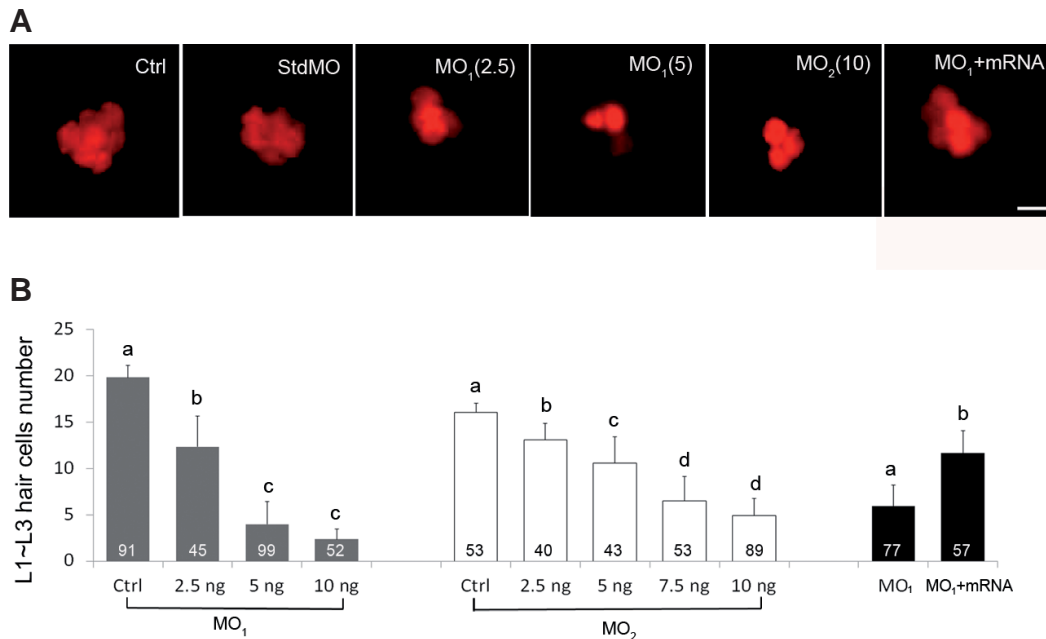


**Fig. 6. Knockdown of calnexin dose-dependently inhibited neuromast hair-cell formation.** *Embryos were treated with different dosages of morpholino and calnexin mRNA are stained with DASPEI instead of WGA488 at 72 hpf to reveal neuromast hair cells. Representative photographs of one neuromast are shown in* **(A)**. *Total hair-cell numbers of the L1~L3 trunk neuromasts in all treatments were counted and are shown in* **(B)**. *Scale bar: 25 μm. The number within each column is the sample size.*
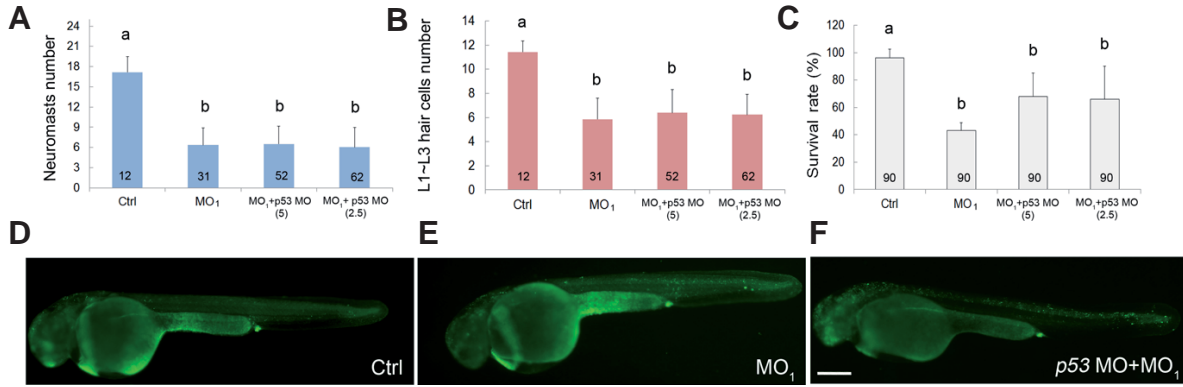
**Fig. 7. *Calnexin* morpholino oligonucleotide (MO)-induced lateral line defects are independent of p53.** *Embryos were treated without (Ctrl) or with 5 ng of the calnexin MO₁ (MO) in the presence or absence of 2.5 or 5 ng of p53 MO until 3 day post-fertilization (dpf). Numbers of trunk neuromasts* **(A)** *and neuromast hair cells* **(B)**, *and the survival rate* **(C)** *are shown. Treated embryos were also stained with the vital dye, acridine orange, at 36 hpf to observe apoptotic cells and photographed under epifluorescent microscopy. Representative photographs for all treatments are shown in lateral view with the anterior to the left and posterior to the right* **(D-F)**. *Scale bar: 200 μm. The number within each column represents the sample size.*

assay. The PLLP cells are more condensed than that of adjacent cells around the primordium, so we could visualize PLLP and count apoptotic cells therein. Twice the number of apoptotic cells in the PLLP was observed in *calnexin* morphants compared to control

embryos (Fig. 9 C,D). In addition, calnexin is thought to be related to the ER stress response and ER stress-induced apoptosis (Guerin *et al.*, 2009, Lee *et al.*, 2006, Zuppini *et al.*, 2002). To determine if the elevation in cell apoptosis in *calnexin* morphants was caused
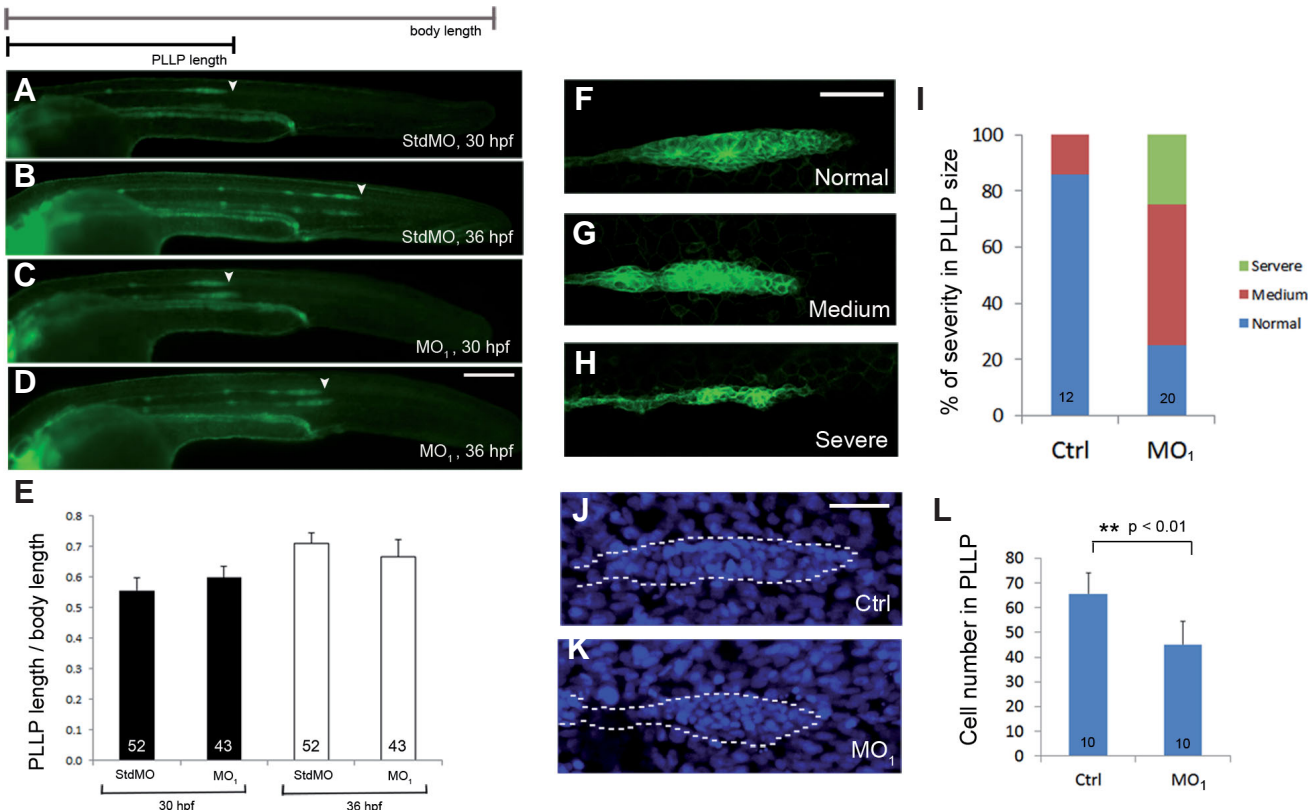


**Fig. 8. Loss of calnexin reduced primordium size but did not affect migration of the posterior lateral line primordium (PLLP). (A-D)** *Transgenic claudin b:gfp embryos were treated with 5 ng std MO and with 3.75 ng of the calnexin MO₁ and imaged at 30 and 36 hpf. Embryos were observed and photographed under epifluorescence microscopy. Scale bar: 200 μm.* **(E)** *Ratios of the migration path of the PLLP to body length at 30 and 36 hpf are shown.* **(F-K)** *Transgenic claudin b:gfp embryos were treated without or with MO₁, cultured until 32 hpf, stained with DAPI and examined under confocal microscopy for GFP (excitation: 455-490 nm; emission 500-540 nm) and DAPI signal (excitation: 350 nm; emission 470 nm), respectively. Representative confocal photographs of different severity of PLLP defects are shown in* **(F-H)** *and the percentages of embryos with different severities are shown in* **(I)**. *Photographs of control embryos* **(J)** *and MO₁ morphants* **(K)** *stained with DAPI are shown.* **(L)** *The average cell numbers in PLLPs are shown.* * *Indicates that the value significantly differs from that of control embryos (p < 0.001). Scale bar: 50 μm. Photographs are shown in lateral view with the anterior to the left and posterior to the right.*
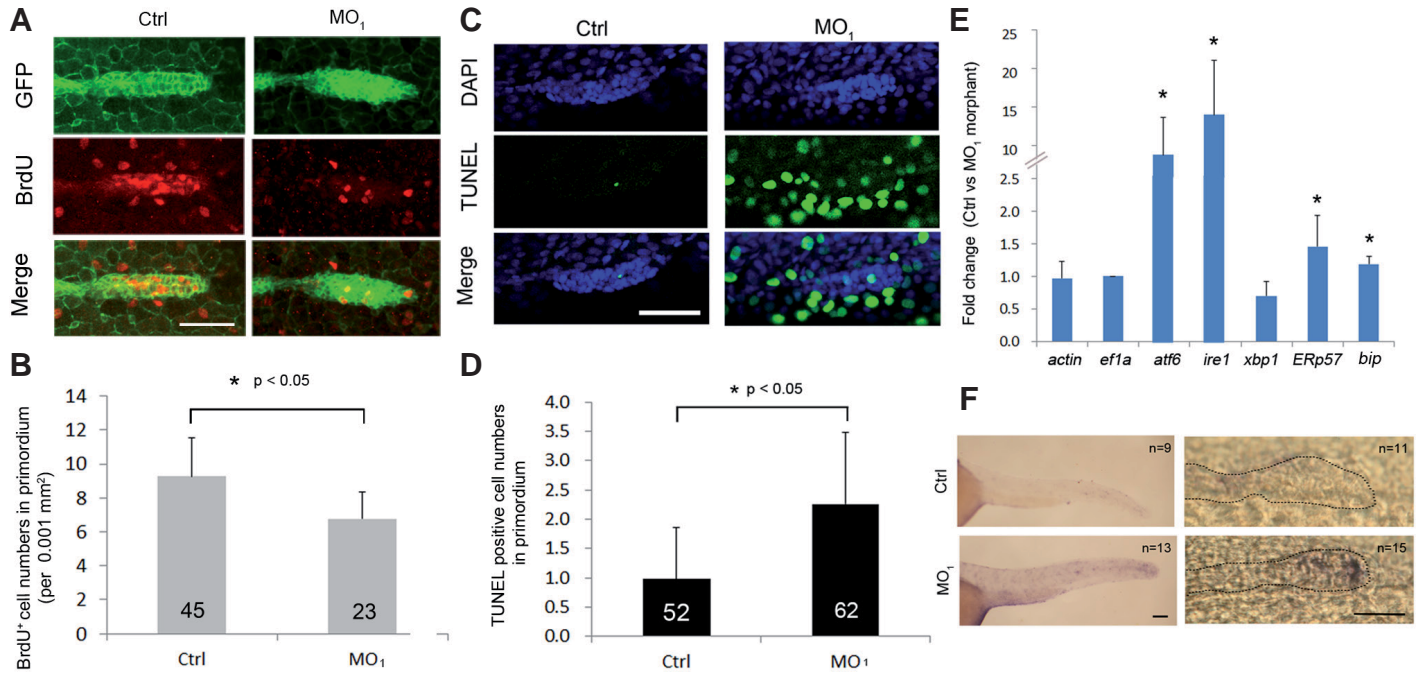
**Fig. 9. Loss of calnexin inhibited cell proliferation and enhanced apoptosis in the posterior lateral line primordium (PLLP). (A)** *Transgenic claudin b:gfp embryos were treated without and with 3.75 ng of the* calnexin *$MO_1$ and collected at 32 hpf. Embryos were labeled with BrdU to reveal proliferating cell and the PLLP was shown by immunostaining against GFP (green). Embryos were examined under confocal microscopy. Photographs are shown in each channel and superimposed images are shown at the bottom.* **(B)** *The proliferation rate was estimated by the average number of BrdU-positive cells per 0.001 mm² of PLLP.* **(C)** *Nuclei of treated embryos were stained with DAPI in blue and apoptotic cells were revealed by a TUNEL staining in green. The average numbers of apoptotic cells in the PLLP are shown in* **(D)**. **(E)** *Embryos were treated as above and subjected to real-time PCR analysis against designated endoplasmic reticular stress-related genes at 36 hpf.* **(F)** *WISH against* bip *was performed and photographed to show the posterior (left) and PLLP (right) regions. Black dotted lines outline the PLLP region. * The value significantly differs from that of control embryos (p < 0.05). Photographs are shown with the anterior to the left. Scale bar: 50 μm.*

by ER stress, we measured changes in expressions of several ER stress genes in 36-hpf embryos (Hu *et al.*, 2007, Kimata and Kohno, 2011, Tabas and Ron, 2011). It showed that expressions of the ER stress genes, *atf6*, *ire-1*, *ERp57,* and *bip,* but not *xbp-1,* were notably elevated in *calnexin* morphants compared to control embryos (Fig. 9E). To further confirm if ER stress is unregulated especially in primordium. We perform WISH analysis to detect the expression of *bip*, which has been used as an ER stress marker in zebrafish embryos (Lin *et al.*, 2011). We observed that the expression of *bip* notably elevated in the whole embryo, including the PLLP, in *calnexin* morphants at 36 hpf (Fig. 9F). Collectively, the reduction in the PLLP size in *calnexin* morphants might have been interfered by both cell proliferation and apoptosis.

## Discussion

Calnexin is known for its calcium-modulation (Michalak *et al.*, 2002) and ER-chaperone activities (Bedard *et al.*, 2005, Zuppini *et al.*, 2002). It is involved in many cellular processes, including immunity, cell adhesion, and development (Gold *et al.*, 2010). Herein, we demonstrate a novel role of calnexin of mediating lateral line development in zebrafish possibly via regulating the expressions of ER stress-response genes to inhibit cell proliferation and increase apoptosis in PLLP.

### Specific expression of calnexin in the lateral line

Despite the conservation of amino acid sequences and functional

domains for zebrafish calnexin compared to its vertebrate homologues, the expression pattern of *calnexin* during development was not previously reported. In this study, we first demonstrated that *calnexin* is expressed in the lateral line system from 36 hpf on. Genes like *cd9b*, *f11r*, *anosmin-1a*, and *neuroD* which are expressed in the PLLP, were all shown to affect lateral line development (Gallardo *et al.*, 2010, Sarrazin *et al.*, 2006, Yanicostas *et al.*, 2008). This implies a role of calnexin in mediating lateral line development or functions.

### Calnexin is required for lateral line neuromast formation

By applying *calnexin* MOs, we clearly demonstrated the necessity for calnexin in lateral line development. This coincides nicely with distinct expression of *calnexin* in the lateral line system. MOs need to be applied with caution due to possible nonspecific secondary effects (Robu *et al.*, 2007). We addressed these issues by first using two non-overlapping MOs with demonstrated efficacy and showed their dose-dependent inhibition of neuromast formation. Next, we eliminated any possible off-target effects by activating p53-dependent cell death (Robu *et al.*, 2007) to show that the reduction in neuromasts and increase in apoptosis were not affected in *calnexin* morphants co-injected with the *p53* MO to block activation of p53. Last, these *calnexin* MO-induced lateral line defects could be rescued by overexpression of *calnexin* mRNA. Collectively, these results unequivocally demonstrate the specificity of the *calnexin* MOs used and their inhibition of development of lateral line neuromasts in zebrafish.

### Loss of calnexin reduces PLLP cell numbers by decreasing cell proliferation and increasing ER-dependent cell apoptosis

The Wnt/β-catenin signaling is central to mediate the cell proliferation in PLLP(Aman *et al.*, 2011). We observed a smaller primordium in *calnexin* morphants (Fig. 8 G,H) with a lower proliferation rate (Fig. 9 A,B).It suggested that calnexin may be involved in the Wnt/β-catenin signaling to regulate the proliferation of PLLP. But it needs more evidences to find the precise role of calnexin in this pathway. Previous studies showed that *eya1 and bap28* mutants are characterized by an increase in cell death in the PLLP that leads to lower proneuromast deposition (Aman and Piotrowski, 2008, Kozlowski *et al.*, 2005). Calnexin is thought to be involved in ER stress-mediated cell apoptosis (Bollo *et al.*, 2010, Zuppini *et al.*, 2002). In *Caenorhabditis elegans*, loss of calnexin caused higher sensitivity to ER stress (Lee *et al.*, 2006). Here, we also demonstrated that ER stress-related genes *atf6*, *ire1*, *ERp57* and *bip* were up regulated in *calnexin* morphants. Similarly, WISH analysis also revealed a systematic elevation of *bip* expression in the whole embryo including PLLP (Fig. 9F). These data suggest a pivotal role of ER stress in mediating PLLP development. No increase in *xbp-1* expression in *calnexin* morphants is puzzling. It might be that ER stress causes splicing of *xbp-1* mRNAs rather than increasing gene expression (Hu *et al.*, 2007). However, no change of splicing pattern in *calnexin* morphants was observed (data not shown). Furthermore, a previous study showed that ER stress participates in blocking Wnt processing and secretion in tumor (Verras *et al.*, 2008). This provides a possible link between ER stress and Wnt pathway, but, the correlation between ER stress and Wnt signaling in zebrafish development still needs further investigation.

Taken together, we demonstrate a novel role of calnexin in regulating zebrafish lateral line development. We also provide evidence that the effect of *calnexin* on the PLLP occurs by modulating ER stress.

## Materials and Methods

### Ethics statement

All animal handling procedures were approved by the Use of Laboratory Animal Committee at National Taiwan University, Taipei, Taiwan (IACUC approval ID: 97 Animal Use document no. 55).

### Fish breeding and embryo collection

AB/Tuebingen and *Tg(-8.0cldnb:lynEGFP)*$^{zf106}$ zebrafish (Haas and Gilmour, 2006) were raised at 28.5 °C under a 14-h/10-h day/night cycle. Fertilized eggs were collected 15 min after natural spawning and incubated in 0.3x Danieau's buffer (1x Danieau's buffer: 58 mM NaCl, 0.7 mM KCl, 0.4 mM $MgSO_4$, 0.6 mM $CaCl_2$, and 5 mM HEPES in double-distilled $H_2O$, with the pH adjusted to 7.6) supplemented with 50 μg/mL streptomycin and 50 μg/mL penicillin G at 28.5 °C until examination or fixation. Embryos were treated with 0.2 mM 1-phenyl-2thiourea in 0.3x Danieau's buffer after 12 hpf to prevent melanin pigment formation if necessary.

### Sequence analysis of calnexin

Homologous calnexin genes were identified from the NCBI database as follows: human, NM_001746.3; mouse, NM_007597.3; rat, NM_172008.2; *Xenopus*, NM_001085946.1; fly, NM_170407.2; nematode, NM_066775.3; and zebrafish, NM_213448.1. Sequence alignment and phylogenetic tree analysis were respectively carried out using ClustalX 1.83 (Thompson *et al.*, 1997) and MEGA 4.3 (Tamura *et al.*, 2007).

### Total RNA isolation and RT-PCR analysis

Total RNAs of embryos at different stages and adult tissues were collected in 1 ml of TheOne™ RNA reagent (Bionovas, Toronto, Canada). Total RNAs were isolated and complementary (c)DNAs were synthesized by incubating the prepared total RNAs, oligo-dT primers and M-MLV reverse transcriptase (Promega, Madison, WI) according to the manufacturer's instructions. Subsequently, 2 μl of cDNA was applied to amplify specific genes according to the following protocol: denaturation at 94 °C for 30 s, annealing at 60 °C for 30 s, and elongation at 72 °C for 45 s (ABI, Veritri™ 96 thermal cycler, Carlsbad, CA). Using the prepared cDNAs, PCRs were performed to amplify *calnexin* and *ef1a* with primer sets listed in Table 1.

### Antisense morpholinos and constructs for ectopic gene expression

All MOs were obtained from Gene Tool (Philomath, OR). Two *calreticulin* translational blocking MOs were used. The first MO, designated $MO_1$ was targeting -6 to +18 of *calreticulin* messenger (m)RNA sequence (NM_131047) with the following sequence: 5'-TGCAGCAGTGATCCG-CATCTCTGC-3'; the second MO, designated $MO_2$ targeted -30 to -6 of the *calreticulin*mRNAwith the following sequence:5'- CACGGTTAAAGGACCT-GCTTTTGAC-3'.Two *calnexin* translation-blocking MOs were used. The first MO, designated $MO_1$, targeted -2 to +23 of the *calnexin* messenger (m)RNA sequence (NM_213448) with the following sequence: 5'-CATA-ACCGCATCTTCAGCTCCATAGT-3'; the second MO, designated $MO_2$, targeted -27 to -2 of *calnexin* mRNA with the following sequence: 5'-TC-CGTGCTTACTGATGTTGCA-3'; a standard control MO (StdMO) (with the sequence 5'-CCTCTTACCTCAGTTACAATTTATA-3') and a *p53*MO (Robu *et al.*, 2007) were also used. The MOs were prepared as 1 mM stocks in sterile double-distilled water, stored at room temperature and diluted in 1x Danieau's buffer with phenol red at the desired concentrations before use.

Full-length *calnexin* cDNA was isolated and subcloned into a pGEMT-easy vector (Promega) by a PCR using primers listed in Table 1. The vector containing *calnexin* was digested with EcoRI and subcloned into a pCS2+ expression vector.

The calnexin expression vector was linearized by XbaI, and capped mRNAs were synthesized by a mMESSAGE Sp6 in vitro transcription kit (Ambion, Austin, TX). The mRNAs were injected into 1-cell-stage embryos at designated concentrations.

### Calnexin and calreticulin translation-blocking MO efficiency check

Partial sequences of *calnexin* (-6 to +339 for $MO_1$ and -33 to +339 for $MO_2$) and *calreticulin* (-18 to +393 for MO) ,which contained respective MO-binding sites, were cloned into the pGEMT-easy vector (Promega), digested with EcoRI and subcloned into the pCS2+-GFP-XLT vector. The translation-blocking activities of the MOs were checked by co-injecting MOs with their respective plasmids, the expression of green fluorescent protein (GFP) was observed at 10 hpf, and the percent of embryos expressing GFP was recorded.

### Microinjection

MOs and/or mRNAs were prepared at desired concentrations in1x Danieau's buffer containing 0.5% phenol red. Injection pipettes were made using 8.9-cm (3.5-in) glass capillaries (World Precision Instrument, Sarasota, FL) pulled by a horizontal puller (P-97, Sutter Instrument, Navato, CA). Microinjection was carried out using a Nanoliter injector (World Precision Instrument). Embryos were immobilized on a 1.2% agar plate during the injection. An injection pipette was forced through the chorion, and 2.3 nL of reagents was injected into the yolk ball and embryo proper for MO and mRNA, respectively.

### Staining of lateral line hair cells

To label neuromast hair cells, embryos were exposed to a vital dye, 4-(4-diethylaminostyryl)-1-methylpyridinium iodine (DASPEI, Sigma, St. Louis, MO) as described previously (Leise, 1996). Embryos at 72~96 hpf were incubated with 0.005% DASPEI in 0.3x Danieau's buffer at room

temperature for 10 min in the dark, and rinsed several times with fresh 0.3x Danieau's buffer to remove the incorporated dye. Embryos were then observed under a DM5000B epifluorescence microscope (Leica, Wetzlar, Germany) using Leica HC PL FLUOTAR objectives and with a rhodamine filter cube then photographed with a CoolSNAPfx CCD camera (Roper Scientific, Tucson, AZ) controlled by Simple PCI Imagine System software (Compix, Sewickley, PA).

To reveal cupula and kinocilia of neuromast hair cells, embryos at 72–96 hpf were incubated in 1 ppm of wheat germ agglutinin conjugated with Alexa Fluor 488 (Invitrogen, Eugene, OR) in 0.3x Danieau's buffer at room temperature for 5 min in the dark, rinsed, and observed as in the DASPEI-staining experiments, but a fluorescein isothiocyanate (FITC) filter cube was used.

### WISH

Embryos were fixed at designated stages in 4% paraformaldehyde (PFA) in phosphate-buffered saline (PBS) at 4 °C overnight, washed several times with PBS, transferred, and stored in 100% methanol at -20 °C for at least 2 h before proceeding. Partial sequences of genes of interest were PCR-cloned into the pGEMT-easy vector using the primer sets listed in Table 1. The respective cDNAs of the above pGEMT-easy clones were used as templates to perform the PCRs using SP6 and T7 primers. The resulting cDNAs were used for in vitro transcription to synthesize digoxigenin (DIG)-labeled probes. WISH was carried out according to standard procedures described by Thisse and Thisse (1993). Images were acquired under a stereoscope (Leica Microsystems, Wetzlar, Germany) and photographed using a Canon EOS 7D camera (Canon, Lake Success, NY). To perform double *in situ* hybridization we first hybridized FITC-labeled *eya1* probe developed with the chromogenic substrates FastRed (Roche Applied Science, Indianapolis, IN, USA) and photographed. Embryos were then stained by DIG-labeled *calnexin* probes as previously described. Images were acquired under Leica DM5000 B DIC microscope (Leica Microsystems, Wetzlar, Germany) and photographed using a Canon EOS 7D camera (Canon, Lake Success, NY).

### Cell proliferation assay

*Tg(-8.0cldnb:lynEGFP)[zf106]* dechorionated embryos were prechilled on ice for 15 min in E3 buffer and transferred to 15% dimethyl sulfoxide (DMSO) in E3 buffer and 15 mM 5-bromo-2'-deoxyuridine (BrdU, Sigma) for 20 min on ice. Embryos were washed several times with E3 buffer and placed at 28.5 °C for 20 min. Embryos were fixed by fresh 4% PFA at room temperature for 2 h, washed several times with PBS, and stored in methanol at -20 °C. Embryos were rehydrated using PBST and treated with 0.01 mg/ml proteinase K in PBST. Embryos were retransferred to 4% PFA for 20 min, washed several times with $H_2O$, and incubated in 2 N HCl for 1 h at room temperature. Embryos were rinsed several times with PBST, blocked with 10% goat serum in PBST for 1 h at room temperature, and incubated with an anti-mouse monoclonal BrdU antibody (1:150 dilution, Roche, Indianapolis, IN) and anti-rabbit polyclonal GFP (1;250, Gene Tex, San Antorinis, Texas) antibody overnight at 4 °C, and then a goat anti-mouse IgG FITC-conjugated secondary antibody (1:2000, Abnova, Taipei, Taiwan), goat anti-rabbit IgG Cy3 conjugated antibody (Abcam, Cambridge, UK) was used as a secondary antibody in 10% goat serum PBST. Embryos photographed and observed by ZEISS LSM 780 confo-

TABLE 1

**PRIMERS USED IN THIS STUDY**

**Primers sets for gene cloning and RT-PCR**

| Oligo Name | Accession No. | Direction | Oligo`s sequence 5` > 3` |
|---|---|---|---|
| *Cloning of full-length Calnexin* | | | |
| calnexin | NM_213448 | forward | 5'-ATGGAACTAAAAATGCGCCTTTGCGTGGC GCTGCTCTCTCT-3' |
| | | reverse | 5'-AAAGAATTCATGGGGGAAGAGGGATGTTG-3' |
| *RT-PCR for detecting gene expression* | | | |
| calnexin | NM_213448 | forward | 5'- AAAAAGCTTCGGACTATGGAGCTGAAGATGC-3' |
| | | reverse | 5'-AAAGAATTCATGGGGGAAGAGGGATGTTG-3' |
| ef1α | NM_200009.2 | forward | 5'-CAAGGAAGTCAGCGCATACA-3' |
| | | reverse | 5'-TGATGACCTGAGCGTTGAAG-3' |
| *Whole-mount in situ hybridization probes* | | | |
| calnexin | | | Same as above |
| bip | NM_213058.1 | forward | 5'- CAGATCTGGCCAAAATGCGG-3' |
| | | reverse | 5'- CTACAGCTCGTCCTTCTCTTCGG-3' |

**Real time primer sets**

| Oligo Name | Accession No. | Direction | Oligo`s sequence 5` > 3` |
|---|---|---|---|
| *Genes for internal control* | | | |
| actin1α | NM_001017750 | forward | 5'- CTCCATCATGAAGTGCGACGT-3' |
| | | reverse | 5'- CAGACGGAGTATTTGCGCTCA-3' |
| ef1α | NM_200009.2 | forward | 5'- CTGGAGGCCAGCTCAAACAT-3' |
| | | reverse | 5'- ATCAAGAGTAGTACCGCTAGCATTAC-3' |
| *ER related genes* | | | |
| atf6 | NM_001110519.1 | forward | 5'-TGTGGACTCACTGTCACCAAA-3' |
| | | reverse | 5'-TGGTTGGAGAGGTTTGGCTTT-3' |
| ER p57 | NM_001199737.1 | forward | 5'-TAAGAACCGCTTCAGCCATGA-3' |
| | | reverse | 5'- CGTATTTGTCTCCTTTGGCTGTT-3' |
| bip | NM_213058.1 | forward | 5'-CGAAGAAGCCAGATATCGATGA-3' |
| | | reverse | 5'-ACGGCTCTTTTCCGTTGAAG-3' |
| ire1 | NM_001020530.1 | forward | 5'-ATGCTGCTGTTGCTGGTTTGC-3' |
| | | reverse | 5'-TACTCGGGAACCTGTATAATG-3' |
| xbp1 | NM_131874.1 | forward | 5'-AAGTCCTCCTGATATCGGGAAAA-3' |
| | | reverse | 5'-TGAAGAGGCTTGATTCGGTATCAT-3' |

cal (Carl Zeiss, Jena, Germany) microscopy. We analyzed the ratio of the number of BrdU positive cells to the area of GFP-labeled primordium using ImageJ software (National Institutes of Health, Bethesda, MD).

### TUNEL assay

Embryos at 32 hpf were fixed overnight with 4% PFA, washed several times with PBST, and stored in 100% methanol at -20 °C. Embryos were rehydrated with a methanol/PBST series, treated with 10 μg/mL proteinase K for 10 min, and then transferred to 4% PFA at room temperature for 20 min. Embryos were incubated in an acetone/ethanol (1:2) mixture for 10 min at -20 °C and washed again in PBST. Apoptotic cells were detected by an In Situ Cell Death Detection Kit, AP (Roche Diagnostics, Indianapolis, IN) according to instructions of the manufacturer. In brief, embryos were incubated with enzyme solutions at 37 °C overnight, washed several times with PBST, observed, and photographed under ZEISS LSM 780 confocal (Carl Zeiss, Jena, Germany) microscopy.

### Cell apoptosis assay by acridine orange staining

Embryos were dechorionated and incubated in a 2 μg/mL solution of *acridine orange* (Sigma) in PBS for 30 min at room temperature. Embryos were washed several times with 0.3x Danieau's buffer and then examined and photographed under epifluorescence microscopy.

### Primordium migration length measurement

To measure the primordium migration path of embryos, we injected designated MOs into embryos from the transgenic *claudin b:gfp* line (*Tg(-8.0cldnb:lynEGFP)$^{zf106}$*), and then incubated and photographed them under epifluorescence microscopy. All experiments were repeated at least three times, and measurements were made using tools in Adobe Photoshop CS4.

### Real-time PCR

RNA from 36-hpf embryos was extracted using the TRIzol reagent (Invitrogen, Carlsbad, CA) and synthesized by M-MLV reverse transcriptase (Promega) with oligo-dT. A qPCR was performed using QuatiFastSYBR Green PCR Master Mix (Qiagen, Valencia, CA). Gene-specific primers were designed by Vector NTI (Invitrogen), and ER-related gene primers are shown in Table 1. Real-time PCR primers for *xbp1*, *hspa5*, and *ER p57* were adapted from Hu *et al.* (2007). All of the data were collected by Bio-Rad iQ5 (Bio-Rad, Hercules, CA).

### Statistical analysis

All experimental values are presented as the mean ± standard error and were analyzed by unpaired-sample Student's *t*-test in Microsoft Excel or analysis of variance (ANOVA) in SAS 9.2 software (SAS, Cary, NC). The number in the bar indicates the total sample number in one experimental condition. Different superscript letters between values indicate a significant difference at $p < 0.05$.

## References

470-482.

AMAN, A. and PIOTROWSKI, T. (2008). Wnt/beta-catenin and Fgf signaling control collective cell migration by restricting chemokine receptor expression. *Dev Cell* 15: 749-761.

BAKER, C.V. and BRONNER-FRASER, M. (2001). Vertebrate cranial placodes I. Embryonic induction. *Dev Biol* 232: 1-61.

BEDARD, K., SZABO, E., MICHALAK, M. and OPAS, M. (2005). Cellular functions of endoplasmic reticulum chaperones calreticulin, calnexin, and ERp57. *Int. Rev. Cytol.* 245: 91-121.

BOLLO, M., PAREDES, R.M., HOLSTEIN, D., ZHELEZNOVA, N., CAMACHO, P. and LECHLEITER, J.D. (2010). Calcineurin interacts with PERK and dephosphorylates calnexin to relieve ER stress in mammals and frogs. *PLoS One* 5: e11925.

BROSAMLE, C. and HALPERN, M.E. (2002). Characterization of myelination in the developing zebrafish. *Glia* 39: 47-57.

DAMBLY-CHAUDIERE, C., CUBEDO, N. and GHYSEN, A. (2007). Control of cell migration in the development of the posterior lateral line: antagonistic interactions between the chemokine receptors CXCR4 and CXCR7/RDC1. *BMC Dev. Biol.* 7: 23.

DAMBLY-CHAUDIERE, C., SAPEDE, D., SOUBIRAN, F., DECORDE, K., GOMPEL, N. and GHYSEN, A. (2003). The lateral line of zebrafish: a model system for the analysis of morphogenesis and neural development in vertebrates. *Biol Cell* 95: 579-587.

DANILCZYK, U.G., COHEN-DOYLE, M.F. and WILLIAMS, D.B. (2000). Functional relationship between calreticulin, calnexin, and the endoplasmic reticulum luminal domain of calnexin. *J Biol Chem* 275: 13089-13097.

DAVID, N.B., SAPEDE, D., SAINT-ETIENNE, L., THISSE, C., THISSE, B., DAMBLY-CHAUDIERE, C., ROSA, F.M. and GHYSEN, A. (2002). Molecular basis of cell migration in the fish lateral line: role of the chemokine receptor CXCR4 and of its ligand, SDF1. *Proc Natl Acad Sci USA* 99: 16297-16302.

DENZEL, A., MOLINARI, M., TRIGUEROS, C., MARTIN, J.E., VELMURGAN, S., BROWN, S., STAMP, G. and OWEN, M.J. (2002). Early postnatal death and motor disorders in mice congenitally deficient in calnexin expression. *Mol Cell Biol* 22: 7398-7404.

FROEHLICHER, M., LIEDTKE, A., GROH, K., LOPEZ-SCHIER, H., NEUHAUSS, S.C., SEGNER, H. and EGGEN, R.I. (2009). Estrogen receptor subtype beta2 is involved in neuromast development in zebrafish (Danio rerio) larvae. *Dev Biol* 330: 32-43.

GALLARDO, V.E., LIANG, J., BEHRA, M., ELKAHLOUN, A., VILLABLANCA, E.J., RUSSO, V., ALLENDE, M.L. and BURGESS, S.M. (2010). Molecular dissection of the migrating posterior lateral line primordium during early development in zebrafish. *BMC Dev. Biol.* 10: 120.

GILMOUR, D., KNAUT, H., MAISCHEIN, H.M. and NUSSLEIN-VOLHARD, C. (2004). Towing of sensory axons by their migrating target cells in vivo. *Nat Neurosci* 7: 491-492.

GOLD, L.I., EGGLETON, P., SWEETWYNE, M.T., VAN DUYN, L.B., GREIVES, M.R., NAYLOR, S.M., MICHALAK, M. and MURPHY-ULLRICH, J.E. (2010). Calreticulin: non-endoplasmic reticulum functions in physiology and disease. *FASEB J.* 24: 665-683.

GUERIN, R., BEAUREGARD, P.B., LEROUX, A. and ROKEACH, L.A. (2009). Calnexin regulates apoptosis induced by inositol starvation in fission yeast. *PLoS One* 4: e6244.

HAAS, P. and GILMOUR, D. (2006). Chemokine signaling mediates self-organizing tissue migration in the zebrafish lateral line. *Dev Cell* 10: 673-680.

HARRIS, J.A., CHENG, A.G., CUNNINGHAM, L.L., MACDONALD, G., RAIBLE, D.W. and RUBEL, E.W. (2003). Neomycin-induced hair cell death and rapid regeneration in the lateral line of zebrafish (Danio rerio). *J Assoc Res Otolaryngol* 4: 219-234.

HU, M.C., GONG, H.Y., LIN, G.H., HU, S.Y., CHEN, M.H., HUANG, S.J., LIAO, C.F. and WU, J.L. (2007). XBP-1, a key regulator of unfolded protein response, activates transcription of IGF1 and Akt phosphorylation in zebrafish embryonic cell line. *Biochem. Biophys. Res. Comm.* 359: 778-83.

KERSTETTER, A.E., AZODI, E., MARRS, J.A. and LIU, Q. (2004). Cadherin-2 function in the cranial ganglia and lateral line system of developing zebrafish. *Dev. Dyn.* 230: 137-143.

KIMATA, Y. and KOHNO, K. (2011). Endoplasmic reticulum stress-sensing mechanisms in yeast and mammalian cells. *Curr. Opin. Cell Biol.* 23: 135-42.

KOZLOWSKI, D.J., WHITFIELD, T.T., HUKRIEDE, N.A., LAM, W.K. and WEINBERG, E.S. (2005). The zebrafish dog-eared mutation disrupts eya1, a gene required for cell survival and differentiation in the inner ear and lateral line. *Dev Biol* 277: 27-41.

AMAN, A., NGUYEN, M. and PIOTROWSKI, T. (2011). Wnt/beta-catenin dependent cell proliferation underlies segmented lateral line morphogenesis. *Dev Biol* 349:

LECAUDEY, V., CAKAN-AKDOGAN, G., NORTON, W.H. and GILMOUR, D. (2008). Dynamic Fgf signaling couples morphogenesis and migration in the zebrafish lateral line primordium. *Development* 135: 2695-2705.

LEE, W., LEE, T.H., PARK, B.J., CHANG, J.W., JR, Y., KOO, H.S., PARK, H., YOO, Y.J. and AHNN, J. (2006). Caenorhabditis elegans calnexin is N-glycosylated and required for stress response (vol 338, pg 1018, 2005). *Biochem. Biophys. Res. Comm.* 341: 895-895.

LEISE, E.M. (1996). Selective retention of the fluorescent dye DASPEI in a larval gastropod mollusc after paraformaldehyde fixation. *Micros. Res. Tech.* 33: 496-500.

LI, Q., SHIRABE, K. and KUWADA, J.Y. (2004). Chemokine signaling regulates sensory cell migration in zebrafish. *Dev Biol* 269: 123-136.

LIN, Y.Y., WHITE, R.J., TORELLI, S., CIRAK, S., MUNTONI, F. and STEMPLE, D.L. (2011). Zebrafish Fukutin family proteins link the unfolded protein response with dystroglycanopathies. *Hum Mol Genet* 20: 1763-1775.

MA, E.Y. and RAIBLE, D.W. (2009). Signaling pathways regulating zebrafish lateral line development. *Curr Biol* 19: R381-R386.

METCALFE, W.K., KIMMEL, C.B. and SCHABTACH, E. (1985). Anatomy of the posterior lateral line system in young larvae of the zebrafish. *J Comp Neurol* 233: 377-389.

MICHALAK, M., GROENENDYK, J., SZABO, E., GOLD, L.I. and OPAS, M. (2009). Calreticulin, a multi-process calcium-buffering chaperone of the endoplasmic reticulum. *Biochem J* 417: 651-666.

MICHALAK, M., ROBERT PARKER, J.M. and OPAS, M. (2002). Ca2+ signaling and calcium binding chaperones of the endoplasmic reticulum. *Cell Calcium* 32: 269-278.

MONTGOMERY, J., CARTON, G., VOIGT, R., BAKER, C. and DIEBEL, C. (2000). Sensory processing of water currents by fishes. *Philos Trans R Soc Lond B Biol Sci* 355: 1325-1327.

NAKAMURA, K., ZUPPINI, A., ARNAUDEAU, S., LYNCH, J., AHSAN, I., KRAUSE, R., PAPP, S., DE SMEDT, H., PARYS, J.B., MULLER-ESTERL, W. *et al.* (2001). Functional specialization of calreticulin domains. *J Cell Biol* 154: 961-972.

NECHIPORUK, A. and RAIBLE, D.W. (2008). FGF-dependent mechanosensory organ patterning in zebrafish. *Science* 320: 1774-1777.

NIXON, S.J., CARTER, A., WEGNER, J., FERGUSON, C., FLOETENMEYER, M., RICHES, J., KEY, B., WESTERFIELD, M. and PARTON, R.G. (2007). Caveolin-1 is required for lateral line neuromast and notochord development. *J Cell Sci* 120: 2151-2161.

OU, W.J., CAMERON, P.H., THOMAS, D.Y. and BERGERON, J.J. (1993). Association of folding intermediates of glycoproteins with calnexin during protein maturation. *Nature* 364: 771-776.

RAIBLE, D.W. and KRUSE, G.J. (2000). Organization of the lateral line system in embryonic zebrafish. *J. Comp. Neurol.* 421: 189-198.

ROBU, M.E., LARSON, J.D., NASEVICIUS, A., BEIRAGHI, S., BRENNER, C., FARBER, S.A. and EKKER, S.C. (2007). p53 activation by knockdown technologies. *PLoS Genet* 3: e78.

RODERICK, H.L., LECHLEITER, J.D. and CAMACHO, P. (2000). Cytosolic phosphorylation of calnexin controls intracellular Ca(2+) oscillations via an interaction with SERCA2b. *J Cell Biol* 149: 1235-1248.

ROSENBAUM, E.E., HARDIE, R.C. and COLLEY, N.J. (2006). Calnexin is essential for rhodopsin maturation, Ca2+ regulation, and photoreceptor cell survival. *Neuron* 49: 229-241.

SARRAZIN, A.F., VILLABLANCA, E.J., NUNEZ, V.A., SANDOVAL, P.C., GHYSEN, A. and ALLENDE, M.L. (2006). Proneural gene requirement for hair cell differentiation in the zebrafish lateral line. *Dev Biol* 295: 534-545.

TABAS, I. and RON, D. (2011). Integrating the mechanisms of apoptosis induced by endoplasmic reticulum stress. *Nature Cell Biol.* 13: 184-190.

TAMURA, K., DUDLEY, J., NEI, M. and KUMAR, S. (2007). MEGA4: Molecular Evolutionary Genetics Analysis (MEGA) software version 4.0. *Molec. Biol. Evol.* 24: 1596-1599.

THISSE, C., THISSE, B., SCHILLING, T.F. and POSTLETHWAIT, J.H. (1993). Structure of the zebrafish snail1 gene and its expression in wild-type, spadetail and no tail mutant embryos. *Development* 119: 1203-1215.

THOMPSON, J.D., GIBSON, T.J., PLEWNIAK, F., JEANMOUGIN, F. and HIGGINS, D.G. (1997). The CLUSTAL_X windows interface: flexible strategies for multiple sequence alignment aided by quality analysis tools. *Nucleic Acids Res.* 25: 4876-4882.

VALENTIN, G., HAAS, P. and GILMOUR, D. (2007). The chemokine SDF1a coordinates tissue migration through the spatially restricted activation of Cxcr7 and Cxcr4b. *Curr Biol* 17: 1026-1031.

VERRAS, M., PAPANDREOU, I., LIM, A.L. and DENKO, N.C. (2008). Tumor hypoxia blocks Wnt processing and secretion through the induction of endoplasmic reticulum stress. *Mol Cell Biol* 28: 7212-7224.

YANICOSTAS, C., ERNEST, S., DAYRAUD, C., PETIT, C. and SOUSSI-YANICOSTAS, N. (2008). Essential requirement for zebrafish anosmin-1a in the migration of the posterior lateral line primordium. *Dev Biol* 320: 469-479.

ZUPPINI, A., GROENENDYK, J., CORMACK, L.A., SHORE, G., OPAS, M., BLEACKLEY, R.C. and MICHALAK, M. (2002). Calnexin deficiency and endoplasmic reticulum stress-induced apoptosis. *Biochemistry* 41: 2850-2858.

**Further Related Reading, published previously in the *Int. J. Dev. Biol.***

**The zebrafish *sf3b1b460* mutant reveals differential requirements for the *sf3b1* pre-mRNA processing gene during neural crest development**
Min An and Paul D. Henion
Int. J. Dev. Biol. (2012) 56: 223-237

**CXCL14 expression during chick embryonic development**
Christopher T. Gordon, Christine Wade, Inigo Brinas and Peter G. Farlie
Int. J. Dev. Biol. (2011) 55: 335-340

**Development of the posterior lateral line system in *Thunnus thynnus*, the atlantic blue-fin tuna, and in its close relative *Sarda sarda***
Alain Ghysen, Kevin Schuster, Denis Coves, Fernando de la Gandara, Nikos Papandroulakis and Aurelio Ortega
Int. J. Dev. Biol. (2010) 54: 1317-1322

**Developmental expression and regulation of the chemokine CXCL14 in *Xenopus***
Byung-Yong Park, Chang-Soo Hong, Faraz A. Sohail and Jean-Pierre Saint-Jeannet
Int. J. Dev. Biol. (2009) 53: 535-540

**Expression of *FoxP2* during zebrafish development and in the adult brain**
Rina Shah, Olga Medina-Martinez, Li-Fang Chu, Rodney C. Samaco and Milan Jamrich
Int. J. Dev. Biol. (2006) 50: 435-438

**Scale development in fish: a review, with description of sonic hedgehog (shh) expression in the zebrafish (Danio rerio)**
Jean-Yves Sire and Marie-Andrée Akimenko
Int. J. Dev. Biol. (2004) 48: 233-247

**Retinoic acid repatterns axolotl lateral line receptors**
Melissa A Gibbs and R Glenn Northcutt
Int. J. Dev. Biol. (2004) 48: 63-66

**Development of axon pathways in the zebrafish central nervous system**
Jensen Hjorth and Brian Key
Int. J. Dev. Biol. (2002) 46: 609-619

**Pathways in blood and vessel development revealed through zebrafish genetics**
Philip S Crosier, Maggie L Kalev-Zylinska, Christopher J Hall, Maria Vega C Flores, Julia A Horsfield and Kathryn E Crosier
Int. J. Dev. Biol. (2002) 46: 493-502

THE INTERNATIONAL JOURNAL OF
DEVELOPMENTAL BIOLOGY
Volume 55 Nos. 7/8/9    Special Issue
Mammary Gland in Development & Cancer

THE INTERNATIONAL JOURNAL OF
DEVELOPMENTAL BIOLOGY
Volume 54 Nos. 6/7    Special Issue
Developmental Hematopoiesis

THE INTERNATIONAL JOURNAL OF
DEVELOPMENTAL BIOLOGY
Volume 56 Nos. 10/11/12    Special Issue
Female Germ Cells in Development & Tumors

THE INTERNATIONAL JOURNAL OF
DEVELOPMENTAL BIOLOGY
Volume 55 Nos. 4/5    Special Issue
Angiogenesis in Development & Cancer